JACS
JOURNAL OF THE AMERICAN CHEMICAL SOCIETY
Article
pubs.acs.org/JACS

Water Promoting Electron Hole Transport between Tyrosine and Cysteine in Proteins via a Special Mechanism: Double Proton Coupled Electron Transfer

Xiaohua Chen,*[,†] Guangcai Ma,[‡] Weichao Sun,[†] Hongjing Dai,[†] Dong Xiao,[†] Yanfang Zhang,[†] Xin Qin,[†] Yongjun Liu,*[,‡] and Yuxiang Bu[‡]

[†]School of Chemistry and Chemical Engineering, Chongqing University, Chongqing, 400030, China
[‡]School of Chemistry and Chemical Engineering, Shandong University, Jinan, Shandong 250100, China

Supporting Information

ABSTRACT: The proton/electron transfer reactions between cysteine residue (Cys) and tyrosinyl radical (Tyr•) are an important step for many enzyme-catalyzed processes. On the basis of the statistical analysis of protein data bank, we designed three representative models to explore the possible proton/electron transfer mechanisms from Cys to Tyr• in proteins. Our ab initio calculations on simplified models and quantum mechanical/molecular mechanical (QM/MM) calculations on real protein environment reveal that the direct electron transfer between Cys and Tyr• is difficult to occur, but an inserted water molecule can greatly promote the proton/electron transfer reactions by a double-proton-coupled electron transfer (dPCET) mechanism. The inserted H_2O plays two assistant roles in these reactions. The first one is to bridge the side chains of Tyr• and Cys via two hydrogen bonds, which act as the proton pathway, and the other one is to enhance the electron overlap between the lone-pair orbital of sulfur atom and the π-orbital of phenol moiety and to function as electron transfer pathway. This water-mediated dPCET mechanism may offer great help to understand the detailed electron transfer processes between Tyr and Cys residues in proteins, such as the electron transfer from Cys_{439} to Tyr_{730}• in the class I ribonucleotide reductase.

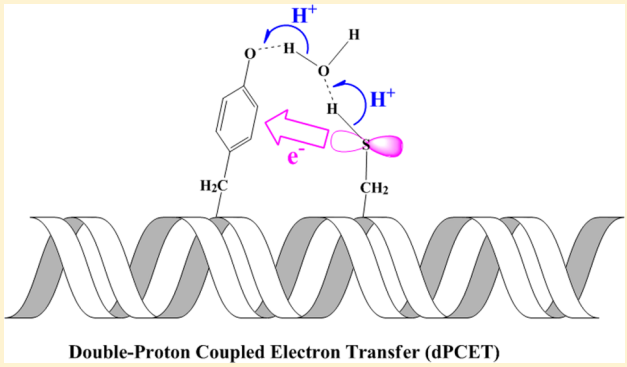

Double-Proton Coupled Electron Transfer (dPCET)

INTRODUCTION

Electron hole migrations in proteins play a critical role in a range of enzymatic processes, such as the reactions of class I ribonucleotide reductase (RNR),[1,2] DNA photolyase,[3] and mitochondrial cytochrome *c* oxidase.[4] A series of intermediate radicals are successively generated during the hole migration processes. Several amino acid radicals, including tryptophanyl (Trp), tyrosinyl (Tyr), and cysteine (Cys) thiyl radicals, have been detected to play significant roles in promoting hole transport. Understanding the fundamental electron transfer mechanisms among these amino acid radicals can gain insight into the details of the corresponding biological processes. Therefore, in the past decade, extensive experimental and theoretical studies have been carried out to investigate the electron transfer mechanisms between Trp and Tyr residues,[5] Tyr and Tyr residues,[6] Trp residue (or Tyr residue) and biologically metal ion centers with different proton acceptors.[7−11] In most situations, electron transfer couples with proton migration to avoid high energy intermediates, which involves the proton-coupled electron transfer (PCET) mechanisms.[12,13] For example, the proton/electron transfer reactions in the model M^{n+}-Tyr complexes (M^{n+} = Ru^{3+},[7,8,10,11] Re^{3+}[9,10]) occur via a bidirection PCET mechanism (*P* = pH < 10) with an electron transfer from the side chain of Tyr to the metal cation and a proton of phenol moiety moving simultaneously to a neighboring base in the different direction. Our recent work has revealed that the proton/electron transfer reactions between Trp and Tyr residues change from the direct PCET mechanism to the proton coupled long-range electron hopping mechanism depending on the peptide conformations in proteins.[5] Compared with these electron transfer systems, however, the electron transfer reactions between Tyr and Cys residues in proteins have been explored to much lesser extent.

The electron transfer between Tyr and Cys residues occurs in many catalytic processes of biological enzymes including the aerobic class I RNR from *Escherichia coli*,[1,2] the myoglobin of the human heart,[14] hemoproteins,[15,16] creatine kinase,[17] parkin,[18] and argininosuccinate synthetase.[19] Stubbe et al. have conducted many important works to confirm that the electron hole migration from Tyr_{731}-Tyr_{730} to Cys_{439} is a key step in the 35 Å long-range radical transfer process of the class I RNR.[1,2,20] In addition, Kalyanaraman and co-workers have revealed that the intramolecular electron transfer from Cys

Received: June 23, 2013
Published: March 6, 2014

   dx.doi.org/10.1021/ja406340z | J. Am. Chem. Soc. 2014, 136, 4515−4524

residue to Tyr radical ($Tyr^{\bullet}$) is very rapid when these two residues are adjacent to each other in proteins and their local environment determines the rate of electron transfer.[16,21] However, the biophysically detailed electron transfer mechanisms between $Tyr^{\bullet}$ and Cys residue in proteins still remain unclear.

Water molecules (H_2Os) are ubiquitous in biomolecules and can affect the electron transfer rate by modulating the electron pathway, as well as changing the energy barrier and the electronic coupling between the donor and acceptor.[22−32] There are two main views about the influence of water on electron transfer in proteins: supporting and prohibiting. In some situations, water chain behaves as a poor electron transfer mediator or appears not to affect on the electron transfer rate significantly.[33−35] In the past few years, however, a number of important experimental[24−28] and theoretical[29−32] investigations emerged to support that a few H_2Os can facilitate protein electron transfer. Most of these observations emphasize that a small number of H_2Os can form water-mediated hydrogen bonds (H-bonds) to link the redox groups, enhance the electronic coupling of donor and acceptor, and lower the energy barrier of electron tunneling.[28,30−32] On the basis of a careful analysis of protein data bank (PDB) structures (such as PDB entries 3N37,[36] 2XO4,[37] 4IHJ[38]), we found that H_2Os may lie around (or between) the side chains of Tyr and Cys residues in proteins. Therefore, H_2Os may influence the electron transfer reactions of these two residues. To the author's knowledge, there is no information available in literature about this issue.

Here, we present a combined density functional theory (DFT) and quantum mechanical/molecular mechanical (QM/MM) investigation on the proton/electron transfer mechanisms between $Tyr^{\bullet}$ and Cys in different cases of proteins. We revealed that water molecule plays a vital role in facilitating electron transfer between $Tyr^{\bullet}$ and Cys and the rate of electron transfer largely depends on the positions of these two residues in the tertiary structures of proteins. Strikingly, a H_2O links the side chains of $Tyr^{\bullet}$ and Cys residues via two intermolecular H-bonds along the water chain, which serves as a proton pathway, and the proton/electron transfer reactions from Cys to $Tyr^{\bullet}$ take place via a double-proton-coupled electron transfer (dPCET) mechanism.

COMPUTATIONAL METHODS

DFT Calculations. All the systems explored in this paper come from a careful analysis of PDB structures. We have identified from 440 electron transport proteins that 26 PDB structures correspond to the case where two close side chains of Tyr and Cys reside at two different peptide chains, and 20 structures contain the two neighboring residues lying in the same alpha-helixes (α-helixes). Considering the effects of dipole moments of α-helixes, the latter class was further subdivided into two categories according to the relative position of these residues in the α-helixes, Cys near the C-terminal (13 entries) and Tyr near the C-terminal (18 entries). On the basis of these cases, we mainly designed three representative models to explore the possible proton/electron transfer mechanisms from Cys to $Tyr^{\bullet}$ in proteins. One is a simple model (Yr-C) including a $Tyr^{\bullet}$ and the side chain of a Cys to illustrate the case where the two adjacent residues lie in two different subunits. The other one is a 14-residue α-helix containing a $Tyr^{\bullet}$ (the fourth residue from the N-terminal) near the N-terminal, a neighboring Cys (the seventh residue from the C-terminal) near the C-terminal, and 12 glycine residues (named as α-YrC). The last one is another 14-residue α-helix, which includes a $Tyr^{\bullet}$ (the seventh residue from the C-terminal) near the C-terminal, a neighboring Cys (the fourth residue from the N-terminal) near the N-terminal and 12 glycine residues (named as α-CYr). The two α-helixes are used to simulate the cases of Tyr and Cys in the same α-helix (or in the same peptide chain) of proteins.

All the calculations on the models above were carried out using the Gaussian 03[39] program package. The UB3LYP[40,41] hybrid functional in conjunction with a 6-311++G(d,p) basis set[42−45] was utilized to fully optimize the geometries of the relative small systems. To reduce computation cost, the large systems were optimized by using the two-layered ONIOM (QM1:QM2) method,[46−54] in which the active center of reactions (H_2Os, the side chains of $Tyr^{\bullet}$ and Cys residues) was treated as the inner layer, and the rest of the system as the outer layer. During the calculations, the full system was called "real" and described at a low level of theory of B3LYP/3-21G(d). The inner layer was termed as "model" and treated by both the low level of theory and a high level of theory of B3LYP/6-311++G(d,p). For all optimized geometries, B3LYP shows essentially no dependence on a change in the size and flexibility of the basis set.

Truhlar and co-workers pointed out that (U)B3LYP calculations underestimate the energy barriers for the radical reactions.[55] However, the MPW1K method, a modified version of the Perdew−Wang gradient corrected exchange functional, could give the best fit to the kinetic data for radical reactions.[55,56] Therefore, the single point calculations at the ONIOM (MPW1K/6-311++g(d,p): MPW1K/3-21G(d)) level were carried out for all large systems. Additionally, an unrestricted second-order Moller−Plesset perturbational theory (MP2) method[57,58] with a 6-31+G(d,p) basis set was used to examine the proton/electron transfer reactions in the simple $Tyr^{\bullet}\cdots$Cys (Yr_C) system. All these validated that the ONIOM (B3LYP/6-311++G(d,p):B3LYP/3-21G(d)) method can give the reliable structures for the interaction between $Tyr^{\bullet}$ and Cys residues in different protein cases. The restricted molecular orbital contours were used to display the orbital character.

PCET rate constants for the proton/electron transfer between $Tyr^{\bullet}$ and Cys in different cases were calculated according to the Marcus−Hush−Levich formula (eq 1).[59−64]

$$k_{\mathrm{PCET}} = \frac{2\pi}{\hbar}\frac{1}{\sqrt{4\pi\lambda k_{\mathrm{B}}T}}|H_{\mathrm{DA}}|^2 \exp\left(-\frac{(\lambda + \Delta G)^2}{4\lambda k_{\mathrm{B}}T}\right) \quad (1)$$

In this expression, λ is the nuclear reorganization energy accompanying electron transfer, H_{DA} is electronic coupling matrix element between the donor and acceptor, ΔG is reaction free energy barrier, $\hbar$ is Planck's constant, k_{B} is Boltzmann's constant, and T is temperature. As the Koopmans theorem (KT) theory, the electronic coupling H_{DA} is related to the energies of the frontier molecular orbitals (MOs) using the structure of the corresponding radical, and it is estimated by eq 2,[65,66]

$$H^0_{\mathrm{DA}} = \frac{\varepsilon_{\mathrm{SOMO}} - \varepsilon_{\mathrm{HDMO\text{-}n}}}{2} \quad (2)$$

where ε_i is energy of the singly occupied MO (SOMO) or the highest doubly occupied MO (HDMO or HDMO-n). HDMO or HDMO-n belongs to an electron donor and SOMO belongs to an acceptor.

QM/MM Calculations. The ONIOM (QM1:QM2) method permits us to treat the relatively large systems at an acceptable computational cost. However, the effect of the surrounding protein environment and solvent water was ignored in the above ONIOM calculations, and some uncertain factors, such as hydrogen bonds and other nonbonding interactions, may play important roles for the proton transfer processes. Therefore, the QM/MM method, which takes effects of entire protein environments and solvents into account, was also carried out for comparison and confirmation of the reliability of the ONIOM(QM1:QM2) method.

The proton/electron transfer reactions from Cys to $Tyr^{\bullet}$ were further investigated by using the combined QM/MM approach according to three protein structures (tubulin tyrosine ligase,[67] lymphoid-specific tyrosine phosphatase,[68] and RNR[37]). In the structure of tubulin tyrosine ligase (F subsection of PDB entry 4IHJ),[67] Tyr_{343} resides at the N-terminal of a 16-peptide α-helix and Cys_{437} does near the C-terminal. This α-helix is used as the initial

dx.doi.org/10.1021/ja406340z | J. Am. Chem. Soc. 2014, 136, 4515−4524

structure for constructing the α-YrC model. In the structure of lymphoid-specific tyrosine phosphatase (PDB code: 4J51),[68] Cys_{238} lies in the N-terminal of a 15-peptide α-helix and Tyr_{242} is near the C-terminal, which is the original structure of α-CYr. The Cys_{439} and Tyr_{730} residues involve the last step of the long-range electron transfer pathway in the first class of RNR[20] (2XO4),[37] as described in the above review. All the proteins were hydrated first using the droplet model with a suitable sphere of equilibrated TIP3 water molecules and then were neutralized by sodium ions at random positions. To equilibrate the prepared system, a series of energy minimizations and an additional 5 ns classical molecular dynamic (MD) simulation were performed using the CHARMM22 force field[69] as implemented in the CHARMM program.[70] The prepared systems served as starting points for the following QM/MM calculations.

The QM/MM calculations were carried out using the ChemShell package[71] integrated with Turbomole program[72] used for the QM treatment and DL-POLY program[73] for handling the MM part of the system using CHARMM22 force field.[69] An electronic embedding scheme[74] was employed for the QM/MM electrostatic interaction with the MM point charges being incorporated into the one-electron Hamiltonian during the QM calculation; i.e., the QM/MM electrostatic interactions were evaluated from all electrons and cores of QM region and the MM partial charges. No cutoffs were introduced for the nonbonding MM and QM/MM interactions. Hydrogen link atoms in combination with the charge shift scheme were applied to treat the QM/MM boundary.[75] The QM/MM geometry optimizations were carried out using the hybrid delocalized internal coordinates (HDLC) optimizer[76] at the B3LYP/6-31G(d,p)//CHARMM level. On the basis of these optimized geometries, high level single-point energy calculations with a larger basis set 6-31++G(d,p) were performed to obtain more accurate energies.

RESULTS

Direct PCET for Close Transoid Arrangement Cys and Tyr•. To investigate the possible proton/electron transfer mechanisms between Tyr• and Cys residue in proteins, we began to examine the hydrogen atom exchange character in the simplest models. The entire possible configurations for the interactions between the side chain of Tyr• and methanthiol have been optimized, and a transoid arrangement (Yr-C) is calculated to be the most stable configuration (Figure S12, Supporting Information), which may represent the case that Tyr• and Cys residues reside at the different peptide chains in proteins. An intermolecular hydrogen bond (H-bond) is formed between the oxygen atom (O atom) of phenoxyl radical and sulfur−H (S−H) bond with a binding strength of 2.8 kcal/mol. The corresponding transoid transition state (Yr-C^{TS}, Figure 1) lies 9.1 kcal/mol in energy above the prereaction complex Yr-C. At the transition state, SOMO is a π-type antibonding interaction involving a delocalized π orbital of the phenol fragment and a 3p atomic orbital of S atom of methanthiol, orthogonal to the O···H···S line. However, its HDMO displays π-bonding character to contact the O atom of phenol and the S atom of methanthiol. Therefore, the interaction of SOMO and HOMO causes a net bonding between the O atom of phenol and S atom of methanthiol, acting as the pathway of electron transfer. However, the proton of S atom migrates along the S···H···O line as shown in Figure 1. In conclusion, the proton/electron transfer reactions between Tyr• and methanthiol in this case is a typical PCET mechanism (Scheme 1A), like the phenoxyl/phenol, methoxyl/methanol,[77] and transiod *tert*-butylperoxyl/phenol exchanges.[6] The theoretical PCET rate constant (k_{ET}) for Yr-C is 5.53×10^8 s^{-1}.

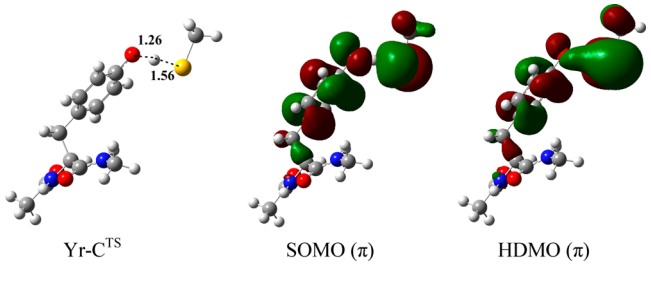

Figure 1. Structure of the transoid transition state of Yr-C (Yr-C^{TS}) with the corresponding singly occupied molecular orbital (SOMO) and the highest double-occupied MO (HDMO). The plot of SOMO delocalized at the side chain of Tyr• and methanthiol displays antibonding character to link the O atom of phenoxyl and S atom, and the plot of HDMO shows a bonding feature.

Water-Assisted dPCET for Close Cys and Tyr• in a α-Helix. In proteins, Tyr and Cys residues may reside at the same peptide chains or the same α-helix with their side chains close to each other (Figure S2, S3, Supporting Information), as mentioned above. It has been reported that the vicinal structures can facilitate the proton/electron transfer reactions between Tyr and Cys residues.[16,21] Therefore, we examined the proton/electron transfer reactions between the two nearby residues lying in the same α-helix according to the structure of α-YrC. The calculation of α-YrC reveals that electron hole mainly localizes on the side chain of Tyr• and the S−H bond does not point to the O atom of phenoxyl (Figure S15, Supporting Information), i.e., there is no intramolecular H-bond between these two side chains. Then, the direct proton/electron transfer reactions from Cys to Tyr• are difficult, and the corresponding transition state can not been found because the rigid framework of the α-helix obstructs the contact of the two side chains. It is in disagreement with the previously reported result that the neighboring Cys and Tyr• structure promotes the proton/electron transfer reaction,[16,21] which arouses us to carry out a further study.

Detailed inspection of protein crystal structures reveals that there are usually water molecules (H_2Os) lying around (or between) the side chains of Tyr and Cys residues.[36−38] We have identified that an entry corresponds to the water-bridged geometry, and 17 entries have H_2Os around side chains of Tyr and Cys residues. H_2Os may play a role in assisting the proton/electron transfer reactions for these two vicinal residues in proteins. Therefore, a H_2O is inserted between the side chains of Tyr• and Cys on the structure of α-YrC to construct a new model, named as α-YrwC. The optimized structures of reactant and transition state, α-YrwC and α-$YrwC^{TS}$, are displayed in Figure 2. Obviously, the inserted H_2O serves as the proton donor and acceptor synchronously to connect the two side chains of Tyr• and Cys by forming two intermolecular H-bonds in α-YrwC. The distances of these two H-bonds, SH···O and OH···O, are 2.25 and 1.86 Å, respectively. The distance from the S atom of Cys to the C_2 of phenoxyl is 4.44 Å. When the reaction proceeds to transition state, the S···C_2 distance reduces to 3.81 Å, and two protons move concertedly. One proton transfers from the S atom of Cys to the O atom of H_2O, and the other one transfers from the O atom of H_2O to the O atom of phenoxyl side chain. Most (0.79) of SOMO delocalize over the two side chains with an antibonding character and the rest (0.21) do at the C-terminus of α-helix, as shown in Figure 2. This is because the C-terminus of α-helix has a low ionization potential, which can readily capture the electron hole in proteins.[78] HOMO-3 mainly delocalizes over the two side

dx.doi.org/10.1021/ja406340z | J. Am. Chem. Soc. 2014, 136, 4515−4524

Scheme 1. Different Mechanisms for the Proton/Electron Transfer Reactions from Cys to Tyr• in Proteins with Various Microstructures[a]

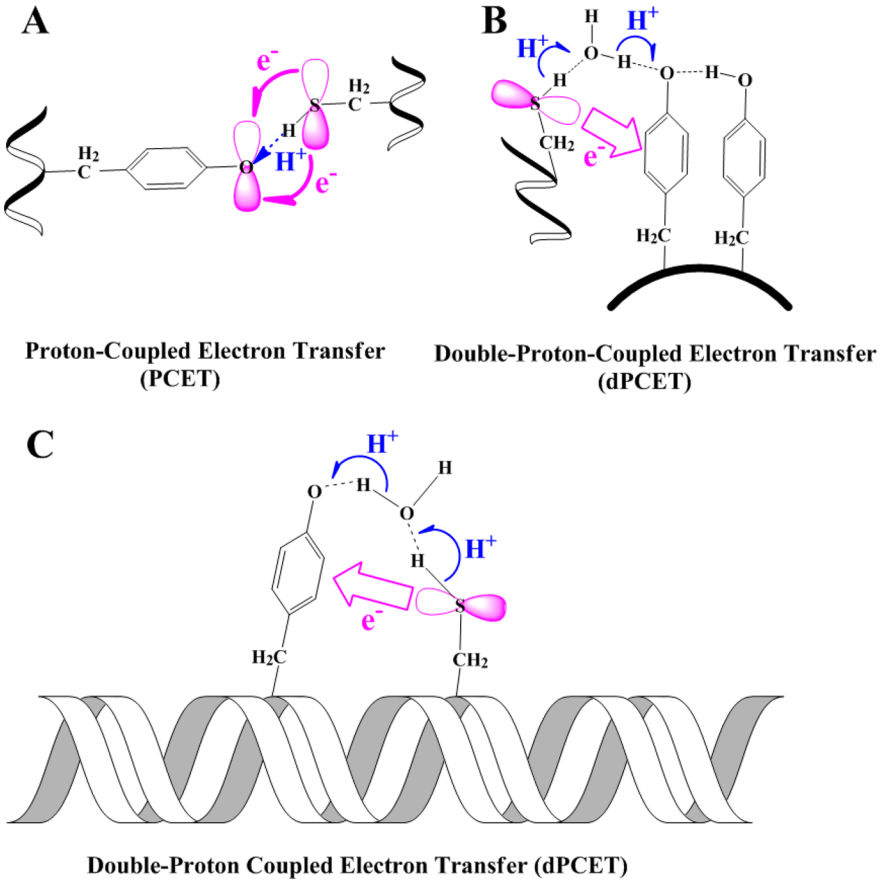

[a](A) Direct proton-coupled electron transfer mechanism (PCET) for the case that the close Cys and Tyr• lie at two different peptide chains in the transoid arrangement. (B,C) The double proton coupled electron transfer mechanism (dPCET) for the cases that a water molecule inserts between two side chains of Cys and Tyr• in proteins.

chains with a bonding character. More importantly, the combination of SOMO and HOMO-3 comes into being a special lp-π three-electron bond (lp ∴ π, lp denotes lone pair) between the S atom and aromatic ring of Tyr,[79] serving as an electron transfer channel. In conclusion, the proton/electron transfer reactions from Cys to Tyr• in α-YrwC follow a dPCET mechanism (Scheme 1C). Besides, the energy of α-YrwC^{TS} is 13.2 kcal/mol higher than that of α-YrwC at the ONIOM-(B3LYP/6-311++G(d,p):B3LYP/3-21G(d)) level of theory with considering zero-point vibrational energy. Moreover, the predicted dPCET rate constant of the α-YrwC system is 1.04×10^5 s^{-1}, which is in agreement with the previously experimental result of $(1.0 \pm 0.6) \times 10^5$ s^{-1}.[80] However, the direct proton/electron transfer reactions can not occur between the side chains of Tyr• and Cys in α-YrC, as mentioned above. Therefore, the inserted H_2O in α-YrwC plays an important role in the activation process of electron transfer by bringing the side chains close to each other.

For comparison with α-YrwC, α-CwYr was also examined in this work. The proton/electron transfer reactions of α-CwYr are similar to that of α-YrwC and follow the dPCET mechanism (Figure S19, Supporting Information). However, the forward barrier of α-CwYr is 17.7 kcal/mol, which is higher than the value of α-YrwC (13.2 kcal/mol). The calculated rate constant (3.34×10^2 s^{-1}) is much smaller than that of α-YrwC (1.04×10^5 s^{-1}), which may be attributed to the influence of dipole moment produced by the electrostatic potential surface of α-helix, in which more negative charges are accumulated at the C-terminus and more positive charges are gathered at the N-terminus in the α-14G, producing a dipole moment along the α-helix from the N-terminus to C-terminus (Figure 3). This dipole moment will undoubtedly retard or promote the electron and proton transfer processes, which depends on the relative direction of the dipole moment to the substance transfer. In the forward reactions of α-YrwC, the proton and electron transfer along with the opposite direction of dipole moment, and the dipole moment will definitely promote the electron transfer and hold back the proton transfer. Moreover, the electron transfer pathway of lp ∴ π three-electron is closer to the α-helix than that of the proton transfer; the dipole moment will impose more influence on the electron transfer and therefore promotes the forward reactions of α-YrwC. In contrary, the dipole moment will inhibit the forward reactions of α-CwYr. As a result, the forward reaction barrier (13.2 kcal/mol) of α-YrwC is lower than that of α-CwYr (17.7 kcal/mol), and the backward reaction barrier of α-YrwC (17.5 kcal/mol) is larger than that (13.6 kcal/mol) of α-CwYr.

In fact, most α-helices have cappings at the C-terminus to counteract the negative charge of the C-terminus in proteins. The C-terminal capping includes the side chains of lysine and arginine residues, H_2Os, and so on.[81] In this work, only the representative side chain of arginine (R) was selected as the C-

dx.doi.org/10.1021/ja406340z | J. Am. Chem. Soc. 2014, 136, 4515−4524

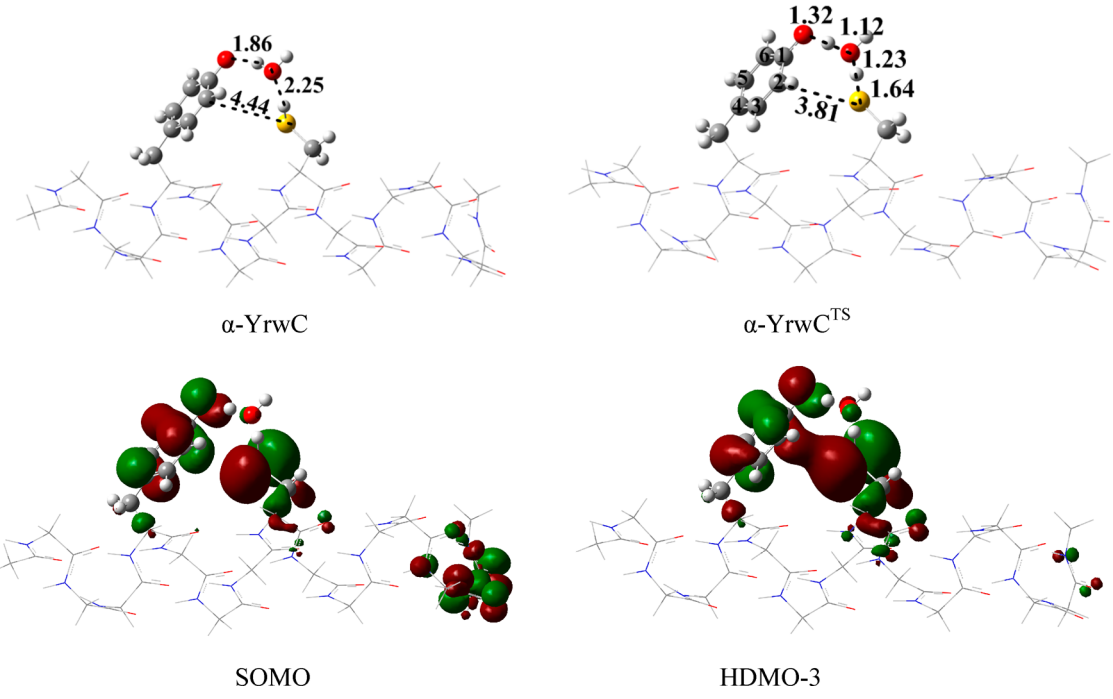

Figure 2. The upper panel shows the structures of α-YrwC and the corresponding transition state α-YrwC^{TS}. The lower panel displays the plots of SOMO and HDMO-3 of the transition state α-YrwC^{TS}.

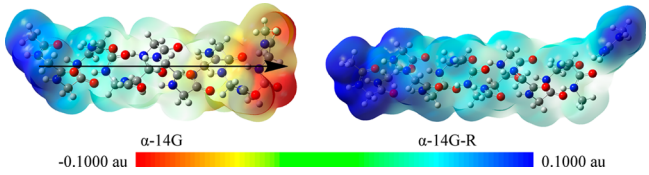

Figure 3. The topologies of electrostatic potential surfaces for α-14G and α-14G-R (14G represents 14 glycine residues and R is the side chain of arginine, a helical cap). The arrow denotes the direction of the dipole moment.

terminal capping of α-YrwC (α-CwYr), named α-YrwC-R (α-CwYr-R). In contrast to α-YrwC, the presence of capping R modulates the distribution of electron hole and energies of MOs. Figure 4 displays that SOMO entirely resides at the side chains of Tyr$^{\bullet}$ and Cys residues at the transition state of α-YrwC-R (α-YrwC-R^{TS}), which is different from the distribution of SOMO in α-YrwC^{TS}. Besides, HDMO-3 in α-YrwC^{TS}, the σ-bonding interaction between the methanthiol and phenoxyl moieties, becomes HDMO in α-YrwC-R^{TS}. However, the proton/electron transfer mechanism of α-YrwC-R is still the same as α-YrwC, proceeding through the dPCET mechanism (Scheme 1C) with a forward barrier of 14.9 kcal/mol. The similar analysis can be made for α-CwYr-R. The details are put in the Supporting Information.

In addition, the side chain (methanol, S) of serine residue has the hydroxyl group, which may have the same function as H_2O for the proton/electron transfer reactions from Cys to Tyr$^{\bullet}$. Therefore, we also examined the system with S instead of the inserted H_2O in α-YrwC-R, named as α-YrSC-R (Figure S22,

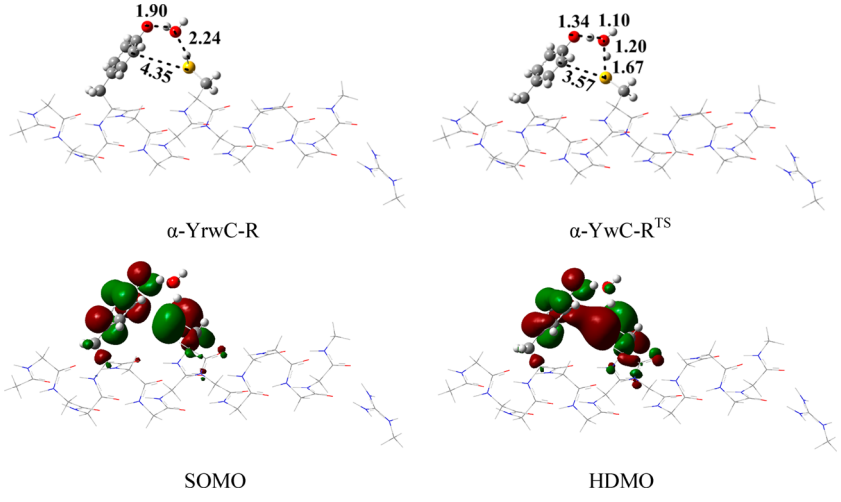

Figure 4. The upper panel shows the structures of α-YrwC-R and the corresponding transition state α-YrwC-R^{TS}. The lower panel displays the plots of SOMO and HDMO of the transition stateα-YrwC-R^{TS}.

dx.doi.org/10.1021/ja406340z | J. Am. Chem. Soc. 2014, 136, 4515−4524

Supporting Information). Our investigations revealed that this substitution does not significantly affect the intramolecular proton/electron transfer reactions from Cys to Tyr• compared to α-YrwC-R. The reactions of α-YrSC-R also occur through the dPCET mechanism with a forward barrier of 12.4 kcal/mol. Therefore, the presence of side chain of Serine can also promote the proton/electron transfer reactions for the vicinal Tyr• and Cys in a α-helix. Besides, the influence of several H_2Os around the side chains of Tyr• and Cys residues in the α-helix was examined. All the calculated results indicate that only the structures with a H_2O lying between the side chains of Tyr• and Cys residues and the other H_2Os around the two side chains are more favorable for the proton/electron transfer from Cys to Tyr•, such as the α-YrwC and α-YrwC-R systems (Table 1 and the Supporting Information).

Table 1. Energy Barrier (E_f^0 and E_b^0) for All Reaction Systems Obtained at the ONIOM(B3LYP/6-311++G(d,p):B3LYP/3-21G(d)), ONIOM(MPW1K6-311++G(d,p):MPW1K/3-21G(d)) and QM(B3LYP/6-31++G)/MM Levels[a]**

species	B3LYP(kcal/mol)		MPW1K (kcal/mol)		QM/MM (kcal/mol)	
ONIOM	E_f^0	E_b^0	E_f^0	E_b^0	E_f^0	E_b^0
Yr-C	9.1	8.7	15.8	12.0		
YrwC	14.2	11.7	16.1	14.0		
α-YrwC	13.2	17.5	20.9	27.1		
α-Yrw$_2$C	12.8	15.6	21.5	26.4		
α-Yrw$_4$C	13.7	15.1	22.6	23.6		
α-CwYr	17.7	13.6	23.3	15.7		
α-YrwC-R	14.9	17.0	20.9	24.7	10.7	11.2
α-YrSC-R	12.4	15.1	17.7	22.3		
α-CwYr-R	14.0	7.8	16.8	8.6	9.1	8.0
YYrwC	8.7	−0.5	9.5	1.0	12.3	10.5

[a]The first two columns include the corresponding zero-point vibrational energies. E_f^0 denotes the forward energy barrier, and E_b^0 represents the backward energy barrier.

To shed light on the effect of biological environment on the proton/electron transfer reactions from Cys to the neighboring Tyr• in a α-helix, we further examined these two residues in two proteins, including tubulin tyrosine ligase (PDB entry 4IHJ)[67] and lymphoid-specific tyrosine phosphatase (PDB entry 4J51),[68] by means of hybrid QM(B3LYP)/MM method. In the QM/MM calculations, according to the structure of 4IHJ, the QM region consists of the side chains of Tyr_{343}• radical, Cys_{347} residue and H_2O, and the MM region contains all the remaining atoms. The optimized structures of reactant (α-$YrwC_R$), transition state (α-YwC_R^{TS}) and product (α-$YwCr_R$) are shown in Figure 5. The H_2O forms two H-bonds with the side chains of Tyr_{343} and Cys_{347} in α-$YrwC_R$ and α-$YwCr_R$ (besides, this H_2O forms another two H-bonds with a neighboring peptide unit and a second H_2O, as shown in the Supporting Information). By comparing with the corresponding structures in Figure 4, it can be seen that the transition state structure obtained by the QM/MM calculations is basically consistent with that from the DFT calculations. More importantly, this consistence indicates that the proton/electron transfer reactions from Cys_{347} to Tyr_{343}• also occur through the dPCET mechanism. However, both the forward and backward energy barriers (10.7 and 11.2 kcal/mol, respectively) are lower than the corresponding DFT results (14.9 and 17.0 kcal/mol), which indicates that the microsurrounding of Cys_{347} and Tyr_{343}• in tubulin tyrosine ligase more favors the dPCET reaction than in the gas phase. The detailed analyses for the proton/electron transfer reactions from Cys_{238} to Tyr_{242}• in the structure of PDB entry 4J51 are put in the Supporting Information. Overall, the QM/MM calculations on the whole protein structures also support that the inserted H_2O facilitates the proton/electron transfer reactions via the dPCET mechanism from Cys to neighbor Tyr• in the same α-helix.

Water-Assisted dPCET for Cys_{439} and Tyr_{730}• in RNR. The interesting involvement of assistant role of H_2O in the Tyr•/Cys proton/electron transfer reactions motivated us to explore the details of reaction mechanism of Tyr_{730}/Cys_{439} couple, which is the last and important step in the well-known 35 Å range radical propagation for the class I of RNR.[2,82] It has been reported that this long-range radical propagation passes through Y_{731} and Y_{730} in α2,[83−85] and the corresponding proton/electron transfer mechanisms between Y_{731} and Y_{730} have been extensively studied.[1,2,6,86] DiLabio et al. proposed that the proton/electron transfer reactions between Tyr_{730} and Tyr_{731} take place via a multiple-centers PCET mechanism with a low energy barrier.[6] More recently, Kaila et al. reported that a H_2O may participate in the Tyr_{730}/Tyr_{731} PCET reactions as an intervening mediator.[86] However, the details of the proton/electron transfer reactions between the Tyr_{730}• radical and the Cys_{439} residue are not clear yet.

Because the three residues Tyr_{731}, Tyr_{730} and Cys_{439} are close, there are two possible proton/electron transfer mechanisms from Cys_{439} to Tyr_{730}/Tyr_{731} radicals. One is a concerted process and the other is a two-step process. For the concerted mechanism, a π-electron and a proton of Tyr_{730}

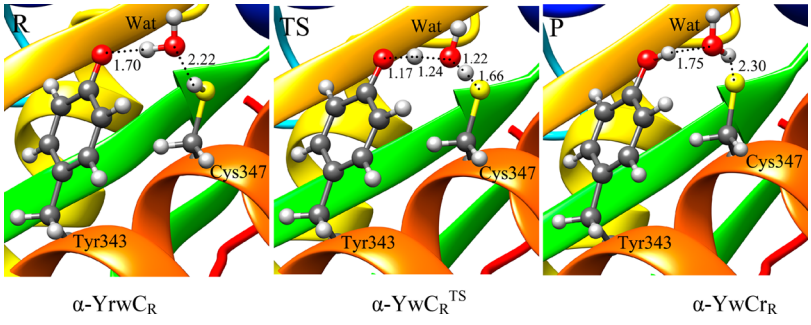

α-$YrwC_R$ α-YwC_R^{TS} α-$YwCr_R$

Figure 5. Optimized structures of reactant (α-$YrwC_R$), transition state (α-YwC_R^{TS}) and product (α-$YwCr_R$) for proton/electron transfer reactions for the two nearby residues lying in a α-helix according to the structure of tubulin tyrosine ligase (PDB entry 4IHJ) at the B3LYP/6-31G(d,p)//CHARMM22 level. Distances are given in Å.

dx.doi.org/10.1021/ja406340z | J. Am. Chem. Soc. 2014, 136, 4515−4524

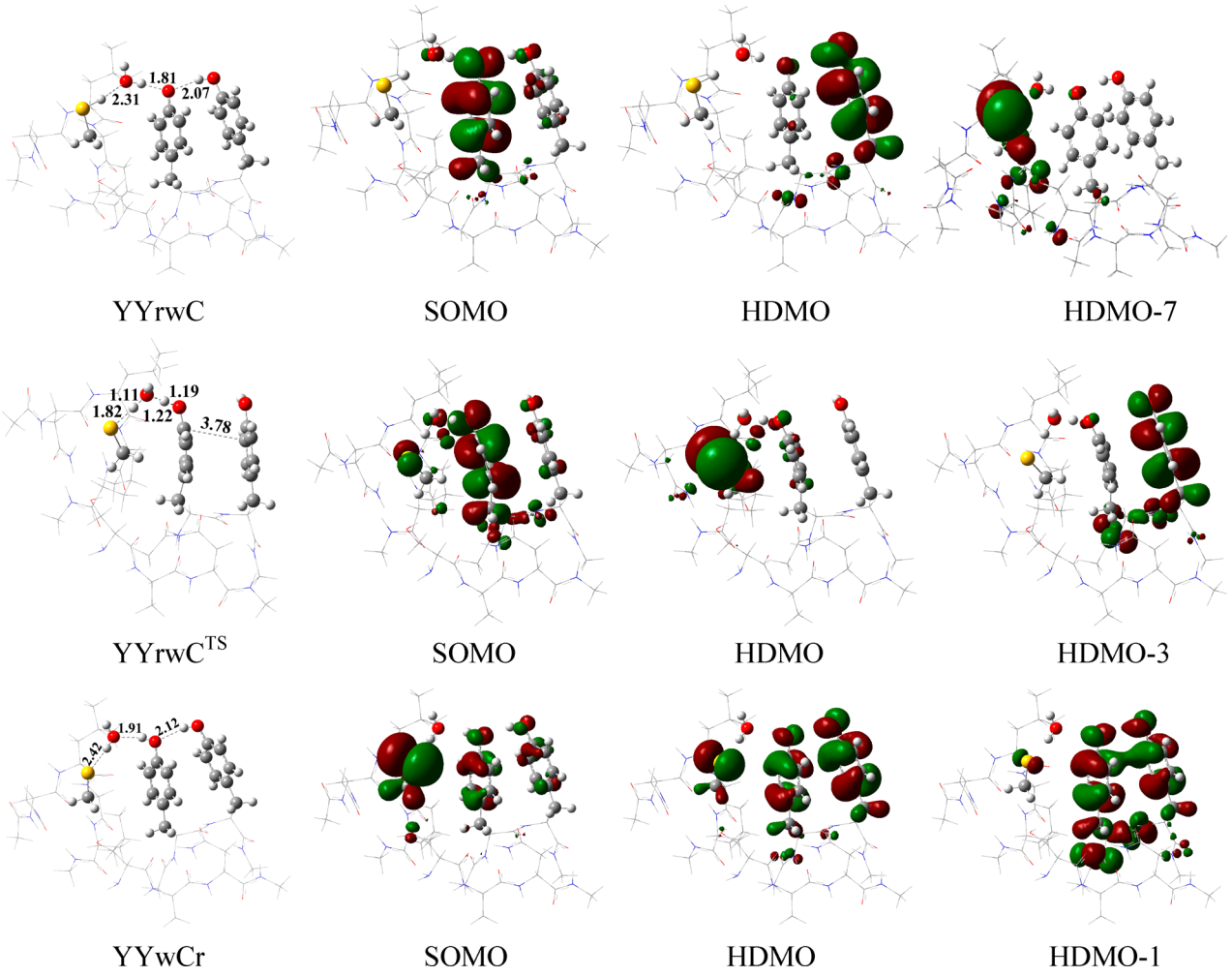

Figure 6. The structures of YYrwC, YYrwC^{TS}, and the YYwCr with the plots of SOMOs, HDMOs and HDMO-ns.

move synchronously to Tyr_{731} radical, and at the same time a lone-pair electron and a proton of Cys_{439} transfer to Tyr_{730}. For the two-step process, the π-electron and the proton of Tyr_{730} first move to Tyr_{731} radical, and then the lone-pair electron and the proton of Cys_{439} shift to Tyr_{730}. Our scanned calculations support the two-step mechanism, as shown in Figure S25 (Supporting Information), agreeing with the previously reported mechanism.[6] However, the energy barrier for the direct proton/electron transfer from Cys_{439} to Tyr_{730} radical is very high (the scanned result is about 60.0 kcal/mol) in the two-step reaction (Figure S26, Supporting Information). Thus, we conjectured that the nearby H_2O (H_2O_{138} in the RNR structure of 2XO4)[37] may also assist the proton/electron transfer from Cys_{439} to $Tyr_{730}^{\bullet}$.

A two-level-ONIOM model was constructed on the basis of the X-ray crystal structure of RNR (pdb 2XO4).[37] In this model, the side chains of Tyr_{731}, $Tyr_{730}^{\bullet}$, and Cys_{439}, and H_2O_{138} are set in high model and the closely related Asn_{437}, Leu_{438}, Leu_{440}, Ser_{694}, Ala_{695} and Asn_{696} and all peptide frameworks are set in low model (the details are described in the Supporting Information). In the RNR structure, H_2O_{138} does not lie between the side chains of Tyr_{730}, and Cys_{439}. But after full optimization, it moves spontaneously into the midst of the two side chains. The optimized structures of the reactant YYrwC, transition state YYrwC^{TS} and product YYwCr, as well as the plots of three relative frontier MOs of all species are shown in Figure 6. For YYrwC, the electron hole mainly resides at the side chain of Tyr_{730}, and HDMO does not localize on the side chain of Cys_{439}, but on the side chain of Tyr_{731}. The lone-pair orbital of the S atom is HDMO-7, which is not the most favorable electron donor than that of π-orbital of Tyr_{731}. However, when the reaction progresses toward transition state, the energies of MOs of reactant exchange each other to be a new order at the transition state as shown in Figure 6. Most of SOMOs still reside on the side chain of Tyr_{730}, and only a small part delocalize on the S atom at the transition state, similar to the reactant. However, the energy of SOMO lowers from −3.46 eV (reactant) to −4.64 eV (transition state). In addition, HDMO-7 (lone pair of the S atom) of the reactant becomes HDMO of the transition state, supporting that the electron transfer reaction occurs from the lone-pair orbital of the S atom to the π-orbital of $Tyr_{730}^{\bullet}$ (Figure 6). The distribution of SOMO at the transition state indicates that only partial electron transfer from the S atom of Cyc_{439} to phenol ring of Tyr_{730}. At the same time, two protons move along the same direction: one is from the S atom to the O atom of H_2O_{138} and the other is from the O atom of H_2O_{138} to the O atom of $Tyr_{730}^{\bullet}$. For the product YYwCr, most of SOMOs reside at the side chain of Cys_{439}, and a few part delocalize over the two-phenol side chains of Tyr_{730} and Tyr_{731}. In contrast, the plots of HDMO and HDMO-1 mainly distribute the two-phenol side chains of Tyr_{730} and Tyr_{731}. The change in distribution of MOs from the

dx.doi.org/10.1021/ja406340z | J. Am. Chem. Soc. 2014, 136, 4515−4524

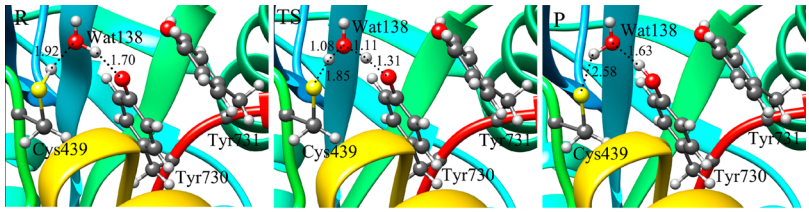

$YYrwC_R$ $YYrwC^{TS}{}_R$ $YYrwCr_R$

Figure 7. Optimized structures of reactant ($YYrwC_R$), transition state ($YYrwC^{TS}{}_R$), and product ($YYrwCr_R$) for the proton/electron transfer reactions between $Tyr_{730}^{\bullet}$ and Cys_{439} residue of RNR (PDB code: 2XO4) at B3LYP/6-31G(d,p)//CHARMM22 level. Distances are given in Å.

reactant to product indicates that the electron transfer reaction occurs from the S atom of Cyc_{439} to the side chains of $Tyr_{730}^{\bullet}$. In conclusion, with H_2O_{138} linking the two side chains of $Tyr_{730}^{\bullet}$ and Cys_{439}, the proton/electron transfer reactions of the active center YYrwC also occur through the dPCET mechanism (Scheme 1B). More importantly, the energy barrier (8.7 kcal/mol) is greatly reduced compared to that of the direct Cys_{439}-Tyr_{730} reactions (about 60.0 kcal/mol), and the predicated dPCET rate constant is 1.38×10^8 s^{-1}. Therefore, during this reaction process, the water molecule (H_2O_{138}) plays a crucial role in facilitating electron transport. H_2O_{138} links the side chains of $Tyr_{730}^{\bullet}$ and Cys_{439} by forming two intermolecular H-bonds to serve as the proton pathway. Furthermore, the inserted H_2O_{138} brings the side chains of Tyr_{730} and Cys_{439} close to each other, enhances the overlap of the π-orbital of phenol and the lone-pair orbital of the S atom, and facilitates the electron transfer from Cys_{439} to $Tyr_{730}^{\bullet}$.

Subsequently, we turned our attention to the actual protein matrixes to scrutinize whether a similar reaction pathway (dPCET) can be accessible in RNR. The structure of $\alpha 2$ in class I of RNR was examined by carrying out the MM and QM/MM computations according to the PDB entity 2XO4. After a 5 ns classical MD simulation, the QM/MM calculations were performed in which the side chains of Cys_{439}, $Tyr_{730}^{\bullet}$, Tyr_{731} and H_2O_{138} were treated as the QM domain and the remaining atoms were assigned to the MM region. All residues and water molecules within 10 Å of $Tyr_{730}^{\bullet}$ remained unrestrained as the active region during the QM/MM geometry optimizations, while the remaining atoms were kept fixed for simplification. It should be noted, in the initial structure of 2XO4, that H_2O_{138} does not lie between the side chains of Cys_{439} and $Tyr_{730,}$ while H_2O_{138} automatically moves to the middle of these two side chains after the QM/MM optimization, agreeing well with the DFT optimized results.[87] The QM(B3LYP)/MM optimized structure of the active site indicates that the two intermolecular H-bonds (1.92 Å for S_{439}–H···O_{138} and 1.70 Å for O_{138}–H···O_{730}, Figure 7) are both shorter than those of the ONIOM model (2.31 and 1.81 Å in YYrwC), revealing that the protein environment can strengthen the H-bond interactions among H_2O_{138} and the side chains of Cys_{439} and $Tyr_{730}^{\bullet}$ to facilitate the double proton transfer. In addition, the structures of the transition state and product obtained by the QM(B3LYP)/MM optimizations are both consistent with the corresponding ONIOM structures (Figure 6 and 7). Therefore, the QM/MM calculations also support that the proton/electron transfer reactions from Cys_{439} to $Tyr_{730}^{\bullet}$ occur through the dPCET mechanism with an assistance of H_2O_{138}. However, the forward and backward energy barriers (12.3 and 10.5 kcal/mol, respectively) are both higher than those of the ONIOM calculations (8.7 and −0.5 kcal/mol). This may be attributed to the fact that the protein environment of RNR greatly stabilizes the $Tyr_{730}^{\bullet}$ and $Cys_{439}^{\bullet}$ radicals. Inspection of the product structure reveals that the side chain of Glu_{441} is near the S atom and the carboxyl group plays an important role in stabilizing the $Cys_{439}^{\bullet}$ radicals. For the $Tyr_{730}^{\bullet}$ radical, besides the close side chains of Tyr_{731}, the side chain of Tyr_{413} is also near the side chain of $Tyr_{730}^{\bullet}$, and the two electron-rich groups make the $Tyr_{730}^{\bullet}$ radical more stable. Therefore, the energy barriers of YYrwC in protein are higher than that of the gas phase.

CONCLUDING REMARKS

In summary, the DFT and QM/MM calculations reveal that the proton/electron transfer reactions between $Tyr^{\bullet}$ and Cys residue depend on the relative positions of these two residues and the assistance of H_2O in proteins. For the case that the close $Tyr^{\bullet}$ and Cys residue reside at different peptide chains, the reactions take place via a typical PCET mechanism with the energy barrier of 9.1 kcal/mol. Unexpectedly, for the cases that these two neighboring residues are in the same α-helix, the direct reactions between $Tyr^{\bullet}$ and Cys are difficult to occur because the rigid structure of α-helix obstructs the H-bond link of the two side chains. However, it is interesting to reveal that an intervening H_2O can promote the proton/electron transfer reactions from Cys to $Tyr^{\bullet}$ through the dPCET mechanism. The intervening H_2O plays two important roles in these reactions: one is to link the electron donor and acceptor via two H-bonds which serves as the proton pathway, and the other is to enhance the overlap between the lone-pair orbital of the S atom and the π-orbital of phenol, which acts as the electron pathway. In addition, our calculations also assist that H_2O_{138} in the class I of RNR promotes the proton/electron transfer reactions between Cys_{439} and $Tyr_{730}^{\bullet}$ by the dPCET mechanism. Our observation is consistent with the previously reported results that a small number of H_2Os inserted between the donor and acceptor in proteins can substantially support electron transfer.[29,30] Furthermore, our investigation reveals the detailed proton/electron transfer mechanisms and elucidates the role of H_2O in the radical transport between Tyr and Cys. The inserted H_2O not only serves as a proton transfer bridges[88] between the electron donor and acceptor, but also plays a vital role in stabilizing both the donor and acceptor while electron and proton synchronously move through different pathways.

ASSOCIATED CONTENT

Supporting Information

The complete citations for refs 39, 69, and 71, as well as the detailed analyses of QM/MM calculations, molecular geometries, orbital characters for all $Tyr^{\bullet}$-Cys complexes and correlations among several quantities. This information is available free of charge via the Internet at http://pubs.acs.org/

dx.doi.org/10.1021/ja406340z | J. Am. Chem. Soc. 2014, 136, 4515−4524

AUTHOR INFORMATION

Corresponding Author

chxh7@cqu.edu.cn; yongjunliu_1@sdu.edu.cn

Notes

The authors declare no competing financial interest.

ACKNOWLEDGMENTS

This work was financially supported by NSFC of China (21003162, 21273291, 21373125, 21173129, 21373123, and 20973101), Science Foundation for The Excellent Youth Scholars of Ministry of Education of China (2103015), Project No. CQDXWL-2012-033 supported by the Fundamental Research Funds for the Central Universities, NSF (ZR2013BM027) of Shandong Province and Project Sponsored by the Scientific Research Foundation of Chongqing University. A part of the calculations were carried out at National Supercomputer Center in Jinan.

REFERENCES

(1) Stubbe, J.; van der Donk, W. A. *Chem. Rev.* **1998**, *98*, 705−762.
(2) Stubbe, J.; Nocera, D. G.; Yee, C. S.; Chang, C. Y. *Chem. Rev.* **2003**, *103*, 2167−2201.
(3) Gindt, Y. M.; Vollenbroek, E.; Westphal, K.; Sackett, H.; Sancar, A.; Babcock, G. T. *Biochemistry* **1999**, *38*, 3857−3866.
(4) Chen, Y.-R.; Gunther, M. R.; Mason, R. P. *J. Biol. Chem.* **1999**, *274*, 3308−3314.
(5) Chen, X.; Zhang, L.; Zhang, L.; Wang, J.; Liu, H.; Bu, Y. *J. Phys. Chem. B* **2009**, *113*, 16681−16688.
(6) DiLabio, G. A.; Johnson, E. R. *J. Am. Chem. Soc.* **2007**, *129*, 6199−6203.
(7) Carra, C.; Iordanova, N.; Hammes-Schiffer, S. *J. Am. Chem. Soc.* **2003**, *125*, 10429−10436.
(8) Sjödin, M.; Styring, S.; Wolpher, H.; Xu, Y.; Sun, L.; Hammarström, L. *J. Am. Chem. Soc.* **2005**, *127*, 3855−3863.
(9) Ishikita, H.; Soudackov, A. V.; Hammes-Schiffer, S. *J. Am. Chem. Soc.* **2007**, *129*, 11146−11152.
(10) Irebo, T.; Reece, S. Y.; Sjödin, M.; Nocera, D. G.; Hammarström, L. *J. Am. Chem. Soc.* **2007**, *129*, 15462−15464.
(11) Bonin, J.; Costentin, C.; Louault, C.; Robert, M.; Savéant, J.-M. *J. Am. Chem. Soc.* **2011**, *133*, 6668−6674.
(12) Hammes-Schiffer, S.; Stuchebrukhov, A. A. *Chem. Rev.* **2010**, *110*, 6939−6960.
(13) Weinberg, D. R; Gagliardi, C. J.; Hull, J. F.; Murphy, C. F.; Kent, C. A.; Westlake, B. C.; Paul, A.; Ess, D. H.; McCafferty, D. G.; Meyer, T. J. *Chem. Rev.* **2012**, *1102*, 4016−4039.
(14) Witting, P. K.; Mauk, A. G. *J. Biol. Chem.* **2001**, *276*, 16540−16547.
(15) Bhattacharjee, S.; Deterding, L. J.; Jiang, J.; Bonini, M. G.; Tomer, K. B.; Ramirez, D. C.; Mason, R. P. *J. Am. Chem. Soc.* **2007**, *129*, 13493−13501.
(16) Bennati, M.; Lendzian, F.; Schmittel, M.; Zipse, H. *Biol. Chem.* **2005**, *386*, 1007−1022.
(17) Arstall, M. A.; Bailey, C.; Gross, W. L.; Bak, M.; Balligand, J. L.; Kelly, R. A. *J. Mol. Cell Cardiol.* **1998**, *30*, 979−988.
(18) Yao, D.; Gu, Z.; Nakamura, T.; Shi, Z. Q.; Ma, Y.; Gaston, B.; Palmer, L. A.; Rockenstein, E. M.; Zhang, Z.; Masliah, E.; Uehara, T.; Lipton, S. A. *Proc. Natl. Acad. Sci. U. S. A.* **2004**, *101*, 10810−10814.
(19) Hao, G.; Xie, L.; Gross, S. S. *J. Biol. Chem.* **2004**, *279*, 36192−36200.
(20) Seyedsayamdost, M. R.; Argirević, T.; Minnihan, E. C.; Stubbe, J.; Bennati, M. *J. Am. Chem. Soc.* **2009**, *131*, 15729−15738.
(21) Zhang, H.; Xu, Y.; Joseph, J.; Kalyanaraman, B. *J. Biol. Chem.* **2005**, *280*, 40684−40698.
(22) Beratan, D. N.; Onuchic, J. N. *Protein Electron Transfer*; Bendall, D. S., Ed.; BIOS Scientific Publishers, Ltd.: Oxford, 1996; p 23.
(23) Berg, J. M.; Stryer, L.; Tymoczko, J. L. *Biochemistry*, 5th ed.; Freeman: New York, 2002.
(24) Page, C. C.; Moser, C. C.; Chen, X.; Dutton, P. L. *Nature* **1999**, *402*, 47−52.
(25) Osyczka, A.; Moser, C. C.; Daldal, F.; Dutton, P. L. *Nature* **2004**, *427*, 607−612.
(26) Francisco, W. A.; Wille, G.; Smith, A. J.; Merkler, D. J.; Klinman, J. P. *J. Am. Chem. Soc.* **2004**, *126*, 13168−13169.
(27) Chakrabarti, S.; Parker, M. F. L.; Morgan, C. W.; Schafmeister, C. E.; Waldeck, D. H. *J. Am. Chem. Soc.* **2009**, *131*, 2044−2045.
(28) de la Lande, A.; Babcock, N. S.; Řezáč, J.; Sanders, B. C.; Salahub, D. R. *Proc. Natl. Acad. Sci. U. S. A.* **2010**, *107*, 11799−11804.
(29) Lin, J.; Balabin, I. A.; Beratan, D. N. *Science* **2005**, *310*, 1311−1313.
(30) Miyashita, O.; Okamura, M. Y.; Onuchic, J. N. *Proc. Natl. Acad. Sci. U. S. A.* **2005**, *102*, 3558−3563.
(31) Migliore, A.; Corni, S.; Felice, R. D.; Molinari, E. *J. Phys. Chem. B* **2006**, *110*, 23796−23800.
(32) Balabin, I. A.; Beratan, D. N.; Skourtis, S. S. *Phys. Rev. Lett.* **2008**, *201*, 158102−158104.
(33) Ponce, A.; Gray, H. B.; Winkler, J. R. *J. Am. Chem. Soc.* **2000**, *122*, 8187−8191.
(34) Gray, H. B.; Winkler, J. R. *Q. Rev. Biophys.* **2003**, *36*, 341−372.
(35) Wenger, O. S.; Leigh, B. S.; Villahermosa, R. M.; Gray, H. B.; Winkler, J. R. *Science* **2005**, *307*, 99−102.
(36) Boal, A. K.; Cotruvo, J. A.; Stubbe, J.; Rosenzweig, A. C. *Science* **2010**, *329*, 1526−1530.
(37) Minnihan, E. C.; Seyedsayamdost, M. R.; Uhlin, U.; Stubbe, J. *J. Am. Chem. Soc.* **2011**, *133*, 9430−9440.
(38) Prota, A. E.; Magiera, M. M.; Kuijpers, M.; Bargsten, K.; Frey, D.; Wieser, M.; Jaussi, R.; Hoogenraad, C. C.; Kammerer, R. A.; Janke, C.; Steinmetz, M. O. *J. Cell Biol.* **2013**, *200*, 259−270.
(39) Frisch, M. J.; et al. *Gaussian 03*, Revision C.02; Gaussian, Inc.: Wallingford, CT, 2004.
(40) Becke, A. D. *J. Chem. Phys.* **1993**, *98*, 5648−5652.
(41) Lee, C.; Yang, W.; Parr, R. G. *Phys. Rev. B: Condens. Matter Mater. Phys.* **1988**, *37*, 785−789.
(42) McLean, A. D.; Chandler, G. S. *J. Chem. Phys.* **1980**, *72*, 5639−5648.
(43) Krishnan, R.; Binkley, J. S.; Seeger, R.; Pople, J. A. *J. Chem. Phys.* **1980**, *72*, 650−654.
(44) Clark, T.; Chandrasekhar, J.; Spitznagel, G. W.; Schleyer, P. v. R. *J. Comput. Chem.* **1983**, *4*, 294−301.
(45) Frisch, M. J.; Pople, J. A.; Binkley, J. S. *J. Chem. Phys.* **1984**, *80*, 3265−3269.
(46) Dapprich, S.; Komaromi, I.; Byun, K. S.; Morokuma, K.; Frisch, M. J. *J. Mol. Struct.* **1999**, *462*, 1−21.
(47) Humbel, S.; Sieber, S.; Morokuma, K. *J. Chem. Phys.* **1996**, *105*, 1959−1967.
(48) Kuno, M.; Hannongbua, S.; Morokuma, K. *Chem. Phys. Lett.* **2003**, *380*, 456−463.
(49) Maseras, F.; Morokuma, K. *J. Comput. Chem.* **1995**, *16*, 1170−1179.
(50) Svensson, M.; Humbel, S.; Froese, R. D. J.; Matsubara, T.; Sieber, S.; Morokuma, K. *J. Phys. Chem.* **1996**, *100*, 19357−19363.
(51) Svensson, M.; Humbel, S.; Morokuma, K. *J. Chem. Phys.* **1996**, *105*, 3654−3661.
(52) Vreven, T.; Morokuma, K. *J. Comput. Chem.* **2000**, *21*, 1419−1432.
(53) Vreven, T.; Mennucci, B.; da Silva, C. O.; Morokuma, K.; Tomasi, J. *J. Chem. Phys.* **2001**, *115*, 62−72.
(54) Vreven, T.; Morokuma, K.; Farkas, O.; Schlegel, H. B.; Frisch, M. J. *J. Comput. Chem.* **2003**, *24*, 760−769.
(55) Lynch, B. J.; Fast, P. L.; Harris, M.; Truhlar, D. G. *J. Phys. Chem. A* **2000**, *104*, 4811−4815.
(56) Lingwood, M.; Hammond, J. R.; Hrovat, D. A.; Mayer, J. M.; Borden, T. W. *J. Chem. Theory Comput.* **2006**, *2*, 740−745.
(57) Frisch, M. J.; Head-Gordon, M.; Pople, J. A. *Chem. Phys. Lett.* **1990**, *166*, 281−289.

(58) Head-Gordon, M.; Head-Gordon, T. *Chem. Phys. Lett.* **1994**, *220*, 122−128.
(59) Marcus, R. A. *J. Chem. Phys.* **1965**, *43*, 679−701.
(60) Hush, N. S. *Trans. Faraday Soc.* **1961**, *57*, 557−580.
(61) Levich, V. G. *Adv. Electrochem. Electrochem. Eng.* **1966**, *4*, 249−371.
(62) Marcus, R. A.; Sutin, N. *Biochim. Biophys. Acta* **1985**, *811*, 265−322.
(63) Costentin, C.; Evans, D. H.; Robert, M.; Savéant, J.-M.; Singh, P. S. *J. Am. Chem. Soc.* **2005**, *127*, 12490−12491.
(64) Schrauben, J. N.; Cattaneo, M.; Day, T. C.; Tenderholt, A. L.; Mayer, J. M. *J. Am. Chem. Soc.* **2012**, *134*, 16635−16645.
(65) Nelsen, S. F.; Weaver, M. N.; Bally, T.; Yamazaki, D.; Komatsu, K.; Rathore, R. *J. Phys. Chem. A* **2007**, *111*, 1667−1678.
(66) Datta, A.; Mohakud, S.; Pati, S. K. J. *Mater. Chem.* **2007**, *17*, 1933−1938.
(67) Prota, A. E.; Magiera, M. M.; Kuijpers, M.; Bargsten, K.; Frey, D.; Wieser, M.; Jaussi, R.; Hoogenraad, C. C.; Kammerer, R. A.; Janke, C.; Steinmetz, M. O. *J. Cell Biol.* **2013**, *200*, 259−270.
(68) He, Y.; Liu, S.; Menon, A.; Stanford, S.; Oppong, E.; Gunawan, A. M.; Wu, L.; Wu, D. J.; Barrios, A. M.; Bottini, N.; Cato, A. C.; Zhang, Z. Y. *J. Med. Chem.* **2013**, *56*, 4990−5008.
(69) MacKerell, A. D., Jr.; et al. *J. Phys. Chem. B* **1998**, *102*, 3586−3616.
(70) Brooks, B. R.; Bruccoleri, R. E.; Olafson, B. D.; States, D. J.; Swaminathan, S.; Karplus, M. *J. Comput. Chem.* **1983**, *4*, 187−217.
(71) Sherwood, P.; et al. *J. Mol. Struct.: THEOCHEM* **2003**, *632*, 1−28.
(72) Ahlrichs, R.; Bar, M.; Haser, M.; Horn, H.; Kolmel, C. *Chem. Phys. Lett.* **1989**, *162*, 165−169.
(73) Smith, W.; Forester, T. R. *J. Mol. Graph.* **1996**, *14*, 136−141.
(74) Bakowies, D.; Thiel, W. *J. Phys. Chem.* **1996**, *100*, 10580−10594.
(75) de Vries, A. H.; Sherwood, P.; Collins, S. J.; Rigby, A. M.; Rigutto, M.; Kramer, G. J. *J. Phys. Chem. B* **1999**, *103*, 6133−6141.
(76) Billeter, S. R.; Turner, A. J.; Thiel, W. *Phys. Chem. Chem. Phys.* **2000**, *2*, 2177−2186.
(77) Mayer, J. M.; Hrovat, D. A.; Thomas, J. L.; Borden, W. T. *J. Am. Chem. Soc.* **2002**, *124*, 11142−11147.
(78) Chen, X.; Zhang, L.; Zhang, L.; Sun, W.; Zhang, Z.; Liu, H.; Bu, Y.; Cukier, R. I. *J. Phys. Chem. Lett.* **2010**, *1*, 1637−1641.
(79) Chen, X.; Tao, Y.; Li, J.; Dai, H.; Sun, W.; Huang, X.; Wei, Z. *J. Phys. Chem. C* **2012**, *116*, 19682−19688.
(80) Steinmann, D.; Nauser, T.; Beld, J.; Tanner, M.; Günther, D.; Bounds, P. L.; Koppenol, W. H. *Biochemistry* **2008**, *47*, 9602−9607.
(81) Doig, A. J.; Chakrabartty, A.; Klingler, T. M.; Baldwin, R. L. *Biochemistry* **1994**, *33*, 3396−3403.
(82) Uhlin, U.; Eklund, H. *Nature* **1994**, *370*, 533−539.
(83) Seyedsayamdost, M. R.; Xie, J.; Chan, C. T.; Schultz, P. G.; Stubbe, J. *J. Am. Chem. Soc.* **2007**, *129*, 15060−15071.
(84) Seyedsayamdost, M. R.; Stubbe, J. *Methods Enzymol.* **2009**, *462*, 45−76.
(85) Minnihan, E. C.; Seyedsayamdost, M. R.; Stubbe, J. *Biochemistry* **2009**, *48*, 12125−12132.
(86) Kaila, V. R. I.; Hummer, G. *J. Am. Chem. Soc.* **2011**, *133*, 19040−19043.
(87) We also tried to find a transition structure for the direct proton/electron transfer reactions from Cys_{439} to $Tyr_{730}^{\bullet}$ by the QM/MM calculations. However, we failed to find the direct transition state.
(88) Mohammed, O. F.; Pines, D.; Dreyer, J.; Pines, E.; Nibbering, E. T. J. *Science* **2005**, *310*, 83−86.